Journal of the Meteorological Society of Japan, Vol. 75, No. 2, pp. 557–568, 1997

Predictability Variation and Quasi-Stationary States in Simple Non-linear Systems

By Shozo Yamane and Shigeo Yoden

Department of Geophysics, Kyoto University, Kyoto 606-01, JAPAN

(Manuscript received 13 June 1996, in revised form 20 January 1997)

Abstract

Basic dynamics on temporal variations of the atmospheric predictability is investigated both with conceptual models of one- and two-dimensional dynamical systems and with a simplified atmospheric circulation model introduced by Legras and Ghil (1985). As a measure of the predictability, we use the Lorenz index α that gives an ensemble average of the error growth rate for a prescribed time interval (Lorenz, 1965). We try to find the relation between the predictability variation and quasi-stationary (QS) states, which occur when the trajectory of the solution passes near a local minimum point (MP), which is either an unstable stationary point (US) or a non-stationary local minimum point (MIN), in phase space. At a MIN the speed of the trajectory has a local minimum value in phase space (Mukougawa, 1988).

In any one-dimensional dynamical system there is a unique relation that α increases monotonically during QS states. In multi-dimensional dynamical systems, on the other hand, there is not such a relation between α and the QS states. During QS states related to a US, it is possible that α varies in more than one manner; α increases monotonically, decreases monotonically, has a maximum, or has a minimum, depending on the trajectory. During QS states related to a MIN, on the assumption that the trajectory exists close enough to the MIN, α shows one of the four relations mentioned above depending on the property of each MIN.

If we consider trajectories only on the attractor, every QS state related to MP has its own tendency in the variation of α, which is one of the four relations. The same relation as in one-dimensional dynamical systems is found in some chaotic solutions in the Legras and Ghil model, although it seems to be just one of the four possibilities.

1. Introduction

Nowadays it is well known that the atmospheric predictability varies day by day depending on the condition of planetary-scale flow (*e.g.*, Kimoto *et al.*, 1992). Though there are some factors of failure in numerical weather prediction, such as an imperfect prediction model, insufficient observation, growing initial error which is the characteristic of chaos, and so on, the dependence of the initial error growth rate on the condition of the flow is considered to cause the predictability variation. The tendency of the variation of the error growth rate has been investigated with low-order models and suggested to be related to the quasi-stationary (QS) state, which is defined as a period when the speed of the trajectory in phase space remains relatively small (Legras and Ghil, 1985, referred to as LG; Mukougawa, 1988). Weather regimes in the mid-latitude troposphere, such as a blocking regime and zonal regime, seem to be a realization of QS states.

LG investigated the relation between the predictability and weather regimes with a low-order atmospheric circulation model. Locating the stationary points of the model and getting some numerical solutions, they found that QS states of the solution occur at the time when the trajectory of the solution passes near an unstable stationary point or a "ghost", which is a shadow of the stationary point in a nearby parameter range. They also showed that the largest real part of the eigenvalues of the Jacobian matrix of the model, which was used as a measure of the predictability, becomes small before the QS state. LG's idea of the "ghost" was generalized by Mukougawa (1988) by introducing a local minimum point, where the speed of the trajectory has a local minimum value in phase space. The local minimum point is a mathematical definition of the QS state.

Mukougawa *et al.* (1991) investigated the relation between the predictability variation and QS states

using the Lorenz (1963) model with three variables. They regarded the laminar phase in an intermittent chaos solution of the model as the QS state in a Poincaré section and used the Lorenz index as a measure of the predictability. The Lorenz index is an ensemble average of the error growth rate for a prescribed time interval (Lorenz, 1965). They indicated that the Lorenz index increases during the QS state.

It is still an open question whether such relation between the Lorenz index and QS states exists in larger dynamical systems. In this paper we first analyze the relation theoretically with one- two-, and more general multi-dimensional non-linear dynamical systems in Section 2. In Section 3, we investigate dynamical properties of the LG model with 25 variables and their relation to predictability variation. Discussion and conclusions are given in Section 4.

2. Theory

2.1 Definitions

Let us consider an n-dimensional dynamical system:

$$\dot{\boldsymbol{x}} = \boldsymbol{f}(\boldsymbol{x}), \tag{1}$$

where the dot denotes the time derivative operator d/dt. $\boldsymbol{x}(t)$ is a vector $(x_1, x_2, ..., x_n)^{\mathsf{T}}$ and superscript $^{\mathsf{T}}$ indicates transpose.

As the definition of the QS state, we use the concept of the local minimum point (hereafter referred to as MP) that is first introduced by Mukougawa (1988). MP is defined as a point at which $\|\dot{\boldsymbol{x}}\|$ has a local minimum value in the n-dimensional phase space, where $\|\boldsymbol{a}\| = \sqrt{\boldsymbol{a}^{\mathsf{T}}\boldsymbol{a}}$. The MPs consist of stationary points which satisfy $\|\dot{\boldsymbol{x}}\| = 0$ and non-stationary local minimum points(MINs) at which $\|\dot{\boldsymbol{x}}\| \neq 0$. The QS state is defined as a period during which $\|\dot{\boldsymbol{x}}\|$ is less than a prescribed small threshold value. That is, during a QS state the trajectory in phase space is in the neighborhood of an MP, which is either an unstable stationary point (US) or a MIN. In the case of a stable stationary point, however, the stationary state will be attained finally since the trajectory only approaches it and does not depart from it.

As a measure of the predictability, we use the Lorenz index $\alpha(\boldsymbol{x}(t_0), \tau)$ that gives an ensemble average of the error growth rate at an initial state $\boldsymbol{x}(t_0)$ for a prescribed time interval τ(Lorenz, 1965; Mukougawa *et al.*, 1991; Kimoto *et al.*, 1992; Yoden and Nomura, 1993).

For a given solution $\boldsymbol{x}(t)$ of Eq. (1), an error $\boldsymbol{y}(t)$ is assumed to be small enough to obey the tangent linear equation:

$$\dot{\boldsymbol{y}} = \mathsf{J}\boldsymbol{y}, \tag{2}$$

where J is the Jacobian matrix: $J_{ij} = \partial f_i/\partial x_j$. Integrating Eq. (2) from $t = t_0$ to $t = t_0 + \tau$ the solution can be written as

$$\boldsymbol{y}(t_0 + \tau) = \mathsf{M}(\boldsymbol{x}(t_0), \tau)\boldsymbol{y}(t_0), \tag{3}$$

where an $n \times n$ matrix $\mathsf{M}(\boldsymbol{x}(t_0), \tau)$ maps $\boldsymbol{y}(t_0)$ to $\boldsymbol{y}(t_0 + \tau)$. The Lorenz index is defined as the root-mean-square of the error growth rate $\|\boldsymbol{y}(t_0 + \tau)\|/\|\boldsymbol{y}(t_0)\|$ of initially randomly distributed errors during the time interval τ. It can be obtained from the trace of the error covariance matrix $\mathsf{M}\mathsf{M}^{\mathsf{T}}$:

$$\alpha(\boldsymbol{x}(t_0), \tau) \equiv \sqrt{\frac{1}{n}\mathrm{trace}[\mathsf{M}(\boldsymbol{x}(t_0), \tau)\mathsf{M}(\boldsymbol{x}(t_0), \tau)^{\mathsf{T}}]}. \tag{4}$$

The Lorenz index $\alpha(\boldsymbol{x}(t_0), \tau)$ generally depends on both the initial state $\boldsymbol{x}(t_0)$ and the time interval τ, except for linear systems in which α is independent of $\boldsymbol{x}(t_0)$.

2.2 The relation between α and MIN in one-dimensional systems

In a one-dimensional system, there is a unique relationship between the Lorenz index $\alpha(\boldsymbol{x}(t_0), \tau)$ and QS states related to MIN(Mukougawa *et al.*, 1991). Equation (3) can be rewritten as,

$$\begin{aligned} y(t_0 + \tau) &= y(t_0) \exp\left(\int_{t_0}^{t_0+\tau} \frac{df}{dx} dt\right) \\ &= y(t_0) \exp\left(\int_{f(x(t_0))}^{f(x(t_0+\tau))} \frac{df}{f}\right) \\ &= y(t_0)\frac{f(x(t_0 + \tau))}{f(x(t_0))} \\ &= y(t_0)\frac{\dot{x}(t_0 + \tau)}{\dot{x}(t_0)}. \end{aligned} \tag{5}$$

Then, the following relation is derived:

$$\alpha = \frac{\|y(t_0 + \tau)\|}{\|y(t_0)\|} = \frac{\dot{x}(t_0 + \tau)}{\dot{x}(t_0)}. \tag{6}$$

The Lorenz index α is less than 1 while the solution $\boldsymbol{x}(t)$ is approaching a MIN, because $\|\dot{x}(t_0)\| > \|\dot{x}(t_0 + \tau)\|$. On the other hand, it is more than 1 while the solution is departing from a MIN, because $\|\dot{x}(t_0)\| < \|\dot{x}(t_0 + \tau)\|$.

By partially differentiating Eq. (6) with respect to t_0 with τ fixed, we obtain the following equation:

$$\frac{\partial \alpha}{\partial t_0} = \left(\left.\frac{df}{dx}\right|_{t=t_0+\tau} - \left.\frac{df}{dx}\right|_{t=t_0}\right)\alpha. \tag{7}$$

Equation (7) indicates that whether α increases or decreases with an increase of t_0 is determined by the sign of $\left(\left.\frac{df}{dx}\right|_{t=t_0+\tau} - \left.\frac{df}{dx}\right|_{t=t_0}\right)$ since $\alpha > 0$. At any MIN $\frac{d}{dt}(\frac{df}{dx}) > 0$, because of an equality,

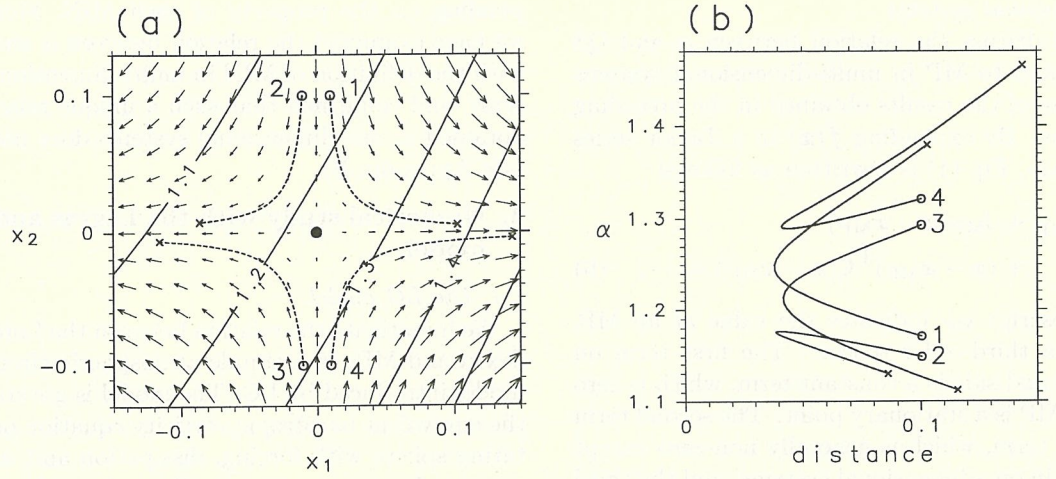

Fig. 1. (a) Distribution of the Lorenz index α for $\tau = 0.5$ in a two-dimensional non-linear dynamical system. Arrows show the flow field of Eq. (8) and • denotes the US $(0,0)^{\mathsf{T}}$. In each quadrant a solution $x(t)$ is drawn with a broken line from an initial value $(\pm 0.01, \pm 0.1)^{\mathsf{T}}$ denoted by ∘ to $t = 2.4$ denoted by ×. (b) Relation between the Lorenz index $\alpha(\tau = 0.5)$ and the distance of the solution from the US. Numbers and markers are the same as those indicated in (a).

$\frac{d}{dt}(\frac{df}{dx}) = f\frac{d^2f}{dx^2} = \frac{1}{2}\frac{d^2f^2}{dx^2} - (\frac{df}{dx})^2$, and the definition of MIN $\left(\left.\frac{df}{dx}\right|_{\text{at MIN}} = 0 \text{ and } \left.\frac{d^2f^2}{dx^2}\right|_{\text{at MIN}} > 0\right)$. This means that the eigenvalue of J, $\frac{df}{dx}$, which is zero at any MIN, has an increasing tendency when the trajectory passes through the MIN. Then, under the condition that τ is not too large, the following relation is obtained: $\left.\frac{df}{dx}\right|_{t=t_0+\tau} > \left.\frac{df}{dx}\right|_{t=t_0}$, *i.e.* $\frac{\partial\alpha}{\partial t_0} > 0$, when the trajectory exists in the neighborhood of any MIN, or, at least when the trajectory that contains the MIN satisfies $\frac{1}{2}\frac{d^2f^2}{dx^2} > (\frac{df}{dx})^2$ from $t = t_0$ to $t = t_0 + \tau$. Thus it is proved that α increases monotonically during QS states related to MIN in one-dimensional systems.

2.3 The relation between α and US in two-dimensional systems

In two-dimensional systems there exist QS states during which the trajectory approaches a US and departs from it, while they do not exist in one-dimensional systems because the trajectory can not approach US. During QS states related to a US, the Lorenz index α may increase monotonically, decrease monotonically, have a maximum, or have a minimum, depending on the trajectory. These properties of α can be shown with non-linear systems with quadratic terms. The following is an example of such systems:

$$\begin{pmatrix}\dot{x}_1\\ \dot{x}_2\end{pmatrix} = \begin{pmatrix}1 & 0\\ 0 & -1.2\end{pmatrix}\begin{pmatrix}x_1\\ x_2\end{pmatrix} + \begin{pmatrix}x_1^2 - 2x_1x_2\\ x_2^2 - 2x_1x_2\end{pmatrix}, \quad (8)$$

which has the dissipative character that the volume decreases in time at a constant rate according to $\nabla\cdot\boldsymbol{f} = -0.2$. The coefficients of the quadratic terms are chosen to satisfy $\nabla\cdot\boldsymbol{f}_{\text{quadratic}} = 0$. The two-dimensional system (8) has a US at $x_1 = x_2 = 0$.

The behavior of α in the neighborhood of the US $(0,0)^{\mathsf{T}}$ is examined for a given τ. Figure 1a shows the distribution of the Lorenz index α for $\tau = 0.5$ in the two-dimensional phase space; contour lines show the dependence of α on the initial state $\boldsymbol{x}(t_0)$. The Lorenz index α is large in the fourth quadrant while it is small in the second quadrant. This dependence results from the quadratic non-linearity; in the case of any linear systems, α is independent of $\boldsymbol{x}(t_0)$. To examine the temporal variation of α along a trajectory $\boldsymbol{x}(t)$ we consider four examples with initial values $(\pm 0.01, \pm 0.1)^{\mathsf{T}}$ indicated by broken lines in Fig. 1a. Each trajectory approaches the US denoted by a bullet at the beginning and departs from it afterward. Figure 1b shows the relation between α and the distance of each trajectory from the US. In contrast with one-dimensional systems, α is not less than 1 while the trajectory is approaching the US. Moreover, the relation obtained in one-dimensional systems holds only in the first quadrant as shown by the solution 1; α increases monotonically during the QS state. In the other three quadrants, this relation does not hold; α decreases monotonically in the third quadrant, has a maximum when the trajectory is close to the US in the second quadrant, and has a minimum when the trajectory is close to the US in the fourth quadrant.

2.4 The relation between α and MP in multi-dimensional systems

We will discuss the relation between α and QS states related to MP in multi-dimensional systems on the base of the results obtained in the preceding subsections. By expanding $\boldsymbol{f}(\boldsymbol{x})$ in a Taylor series for $\boldsymbol{x} = \boldsymbol{x}_{\mathrm{MP}}$, Eq. (1) is rewritten as follows:

$$\dot{\boldsymbol{x}} = \boldsymbol{f}_{\mathrm{MP}} + \mathsf{J}_{\mathrm{MP}}(\boldsymbol{x} - \boldsymbol{x}_{\mathrm{MP}}) + (\boldsymbol{x} - \boldsymbol{x}_{\mathrm{MP}})^{\mathsf{T}}\mathsf{C}(\boldsymbol{x} - \boldsymbol{x}_{\mathrm{MP}}) + \cdots, \quad (9)$$

where subscript $_{\mathrm{MP}}$ indicates the value at an MP, and C is a third-order tensor. The first term on the right-hand side is a constant term, which is zero when the MP is a stationary point. The second term is a linear term, which is generally non-zero except for a MIN in one-dimensional systems, and the third term is a quadratic term.

The distribution of the Lorenz index α in phase space, such as in Fig. 1a, is expressed as a function of initial state $\boldsymbol{x}(t_0)$ for a fixed time interval τ, and its gradient is directly related to the temporal variation of α along a trajectory. The gradient of α in phase space arises from the non-linear terms, which are the third and the following higher-order terms on the right-hand side of Eq. (9); if the system is linear without these terms, α is constant (*i.e.*, independent of $\boldsymbol{x}(t_0)$). On the other hand, the trajectory in the neighborhood of the MP is basically determined by the constant and the linear terms. Therefore it is possible that the Lorenz index α varies in more than one manner during QS states, when the trajectory exists near an MP, as shown in Fig. 1 for a two-dimensional system.

In the case that the MP is a stationary point ($\boldsymbol{f}_{\mathrm{MP}} = \boldsymbol{0}$) or that the constant term is much smaller than the linear term ($\|\boldsymbol{f}_{\mathrm{MP}}\| \ll \|\mathsf{J}_{\mathrm{MP}}(\boldsymbol{x} - \boldsymbol{x}_{\mathrm{MP}})\|$) for any time, the trajectory can approach the MP along the stable manifold spanned by the matrix J_{MP} and depart from it along the unstable manifold. The Lorenz index α may vary in more than one manner during the QS state related to this MP, because neither the direction of approach nor the direction of departure is fixed uniquely. In the case that the MP is a MIN and satisfies the inequality $\|\boldsymbol{f}_{\mathrm{MP}}\| \gg \|\mathsf{J}_{\mathrm{MP}}(\boldsymbol{x} - \boldsymbol{x}_{\mathrm{MP}})\|$ for some time period, on the other hand, the trajectory approaches the MIN and departs from it almost along the direction of the vector $\boldsymbol{f}_{\mathrm{MP}}$. Then the MIN has its own unique tendency of α during the QS state. An example in two-dimensional system is given in Appendix A.

In one-dimensional systems it was proved in Section 2.2 with the definition of MIN that α increases monotonically during the QS state. From the analyses using a simple two-dimensional system with a MIN, however, it can be shown that such a unique relation does not hold generally; during QS states α may increase monotonically, decrease monotonically, have a maximum, or have a minimum, depending on the property of each MIN. Moreover, we have examined the relation between α and MIN with the definition of MIN in multi-dimensional systems, and confirmed that such a unique relation as obtained in one-dimensional systems does not exist (see Appendix B).

3. Numerical study with the Legras and Ghil model

3.1 The LG model

We investigate the relation between the Lorenz index α and MPs in a simple atmospheric circulation model introduced by LG. The model is governed by the equivalent barotropic vorticity equation on a rotating sphere with forcing, dissipation and surface-topography terms. Its non-dimensional form is as follows:

$$\frac{\partial}{\partial t}(\nabla^2 - r^{-2})\psi + \rho J[\psi, \nabla^2\psi] + J[\psi, \mu(1+h)] = \alpha\nabla^2(\psi^* - \psi), \quad (10)$$

where $\psi(\lambda, \mu, t)$ is the streamfunction, λ the longitude, μ the sine of the latitude, t the time, $\psi^*(\mu)$ the streamfunction for a zonally symmetric forcing, $h(\lambda, \mu)$ the topographic height, ∇^2 the horizontal Laplacian operator, $J[a, b]$ the Jacobian operator, r the external radius of deformation, α^{-1} the relaxation time, and ρ the Rossby number, which measures the relative importance of the non-linear Jacobian term.

The experimental framework and procedure are identical to those given in LG. Equation (10) is discretized through an expansion in spherical harmonics $P_n^m(\mu)e^{im\lambda}$ with a triangular truncation of total wavenumber 9 (T9): $\psi(\lambda, \mu, t) = \sum_{n=0}^{9}\sum_{m=-n}^{n}\psi_n^m(t)P_n^m(\mu)e^{im\lambda}$, where $P_n^m(\mu)$ are associated Legendre functions. The equatorial symmetry and the longitudinal periodicity (mod π) of the flow field are also assumed to reduce the degrees of freedom. The model finally becomes a dynamical system of 25 real variables.

The forcing is a zonal jet given by $\psi^*(\mu) = -\kappa\mu^3$, which has a maximum near the latitude of 50°. The coefficient κ is set to a constant such that the maximum eastward speed in dimension is 60 ms^{-1} for $\rho = 0.2$. The topography is given by the gravest wave mode: $h = 4h_0\mu^2(1-\mu^2)\cos 2\lambda$, and the amplitude is set to $h_0 = 0.1$. Other constants are also identical to those given by LG: $r' = 1100$ km and $\alpha' = 0.05$ day^{-1} (prime denotes a value in dimension). The Rossby number ρ is the principal experimental parameter, which is changed in the range of $0.1 \leq \rho \leq 0.3$. The Rossby number is also a measure of the intensity of the forcing because the

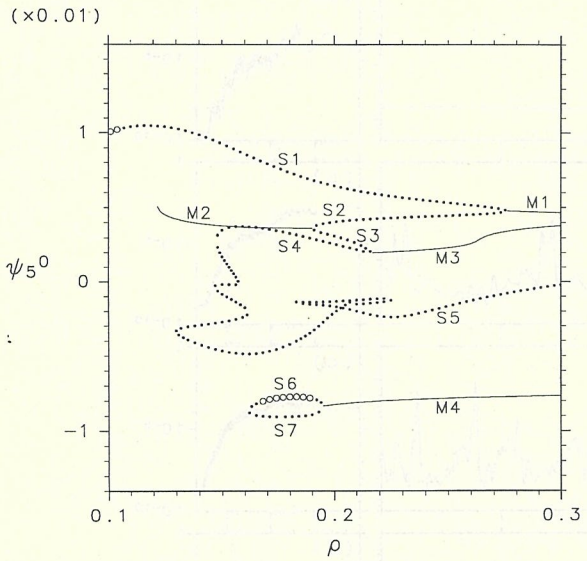

Fig. 2. Dependence of MPs on ρ. The ordinate refers to ψ_5^0 which is one of 25 variables. MPs are classified into stationary points(○:stable, ●:unstable) or MINs(solid line). Some branches are labeled with S(stationary points) or M(MINs).

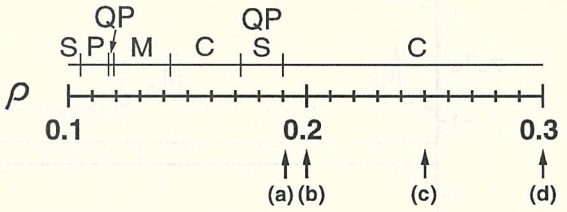

Fig. 3. Dependence of asymptotic solutions on ρ. Symbols represent, respectively, S:stable stationary solution, P:periodic solution, QP:quasi-periodic solution, M:multiple stable solutions, and C:chaotic solution. Points marked with (a)∼(d) indicate the values of ρ for which asymptotic solutions are investigated in detail; (a)ρ = 0.191, (b)0.200, (c)0.250, (d)0.300.

streamfunction is non-dimensionalized by that for the forcing.

3.2 Dynamical structure

Stationary points of the system are obtained by the continuation method similar to LG's while MINs are obtained by the same method as in Mukougawa (1988). Figure 2 shows the dependence of the MPs (stationary points and MINs) on the forcing intensity ρ, adopting ψ_5^0 which is one of the zonal components as the ordinate. All of the branches of stationary points are shown by S1∼S7, most of which are linearly unstable (denoted by dots) in this range of ρ. Although more than 40 branches of MINs are obtained, only four of them are shown (M1∼M4), which are relatively close to the time-dependent solutions obtained numerically. The branch M4 that bifurcates from a limit point of the stationary point branches S6 and S7 corresponds to the "ghost" suggested by LG. The other branches M1∼M3 also have similar structure of bifurcation at a limit point of two stationary point branches.

The asymptotic behavior of time-dependent solutions is investigated by numerical time integrations with the Runge-Kutta-Gill method. Figure 3 summarizes the asymptotic solutions we obtained in the parameter range of $0.1 \leq \rho \leq 0.3$. When ρ is small enough(< 0.106; denoted by S), the solution approaches the stable stationary point S1. As ρ increases, the solution becomes periodic (P), and then quasi-periodic (QP) after a series of Hopf bifurcations at $\rho = 0.106$ and 0.118 as pointed out by LG. The route to chaotic solutions (C) in this system is rather complicated, that is, there is the range of ρ that multiple stable solutions (M) exist, which consist of some periodic and quasi-periodic solutions. Two asymptotic solutions depending on the initial condition are also obtained for the same parameter ρ that is further increased ($0.172 < \rho < 0.190$); a stable stationary solution S6 and a stable quasi-periodic solution. Another type of chaotic solution, which is related to S6 or M4, appears for $\rho > 0.190$.

In the remainder of this section, the four chaotic solutions marked with (a)∼(d) in Fig. 3 are investigated in detail: (a)ρ = 0.191, (b)0.200, (c)0.250, (d)0.300. Figure 4 shows the temporal variation and the power spectral density of $\psi_5^0(t)$ of the solutions. The chaotic solution (a) is characterized by its homoclinic-like behavior, that is, the trajectory recurrently approaches the S6(US) and then departs from it; for example, the trajectory for the first 500-day period in Fig. 4a is closest to the point S6 at day 317. This homoclinic-like behavior is an important structure of the chaotic solutions for $\rho > 0.190$, although S6 is replaced by M4 for $\rho > 0.194$; even in the chaotic solution (d), such recurrent approach and departure are observed. Only the MP of S6 or M4 plays an important role to produce the QS states in these chaotic solutions; no QS state related to other MPs is obtained.

The power spectral density for the chaotic solution (a) shows a red-noise feature with a peak around a period of 400 days, which gives an order of the recurrence time. As ρ increases, high-frequency components have more power; the recurrence time becomes shorter and the temporal variation becomes more irregular.

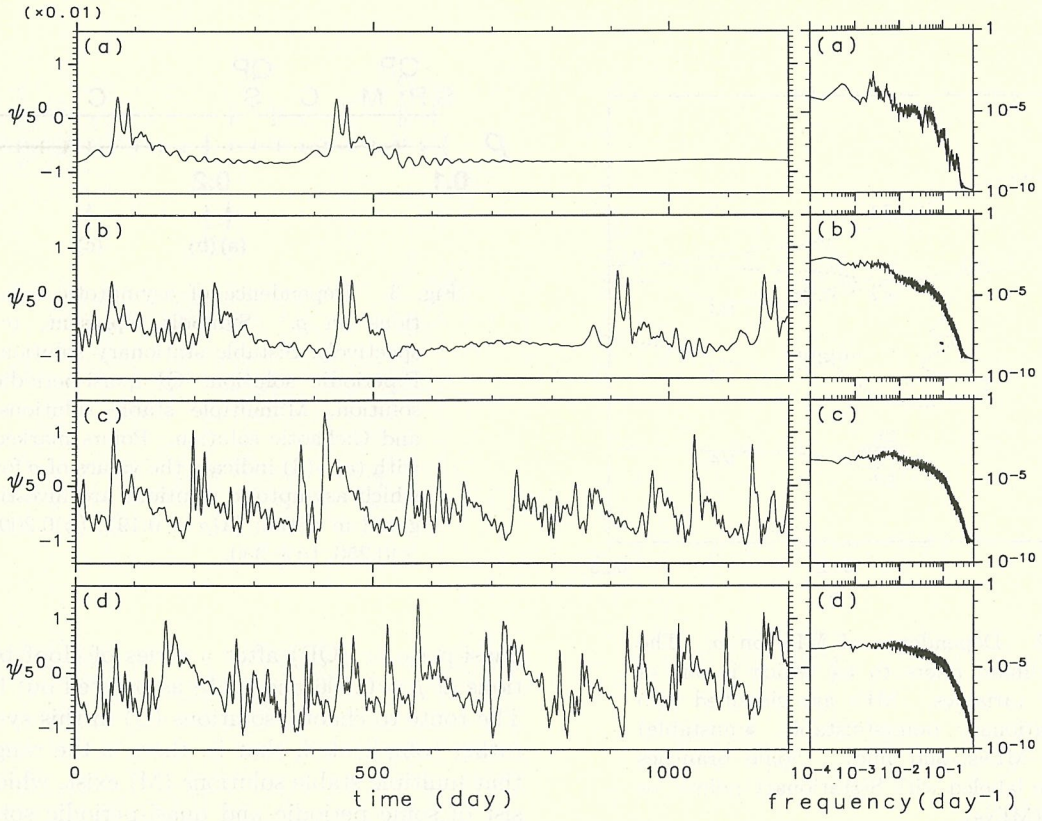

Fig. 4. Temporal variation and power spectral density of $\psi_5^0(t)$. (a)∼(d) are the same as those indicated in Fig. 3.

3.3 The relation between α and MP

Temporal variations of the Lorenz index α along the four chaotic solutions (a)∼(d) are investigated. We choose the root-mean-square of the streamfunction as the norm: $\|\boldsymbol{x}\|^2 = \frac{1}{4\pi}\int_0^{2\pi}\int_{-1}^{1}\psi(\lambda,\mu)^2 d\mu d\lambda$. Figure 5 shows the statistics of the variations of α along each solution $\boldsymbol{x}(t)$ of 9960-day period. Firstly $\alpha(\boldsymbol{x}(t_0),\tau)$ is calculated for 9951 initial states $\boldsymbol{x}(t_0)$ with the sampling time interval of one day for $\tau \leq 10$ days. The geometric mean of α(solid line) shows the characteristics of chaos that it increases almost exponentially with τ. The increment of the mean of α becomes large as ρ increases. The range of α is indicated by two symbols ∘(maximum) and +(minimum) in Fig. 5. The standard deviation of α is also shown in the figure with the shades. Both measures of the temporal variability of α increase as the time interval τ increases. The increment of the variability also becomes large as ρ increases. The largest Lyapunov exponent is also calculated by using Shimada and Nagashima (1979)'s method and shown by a broken line. The geometric mean of α grows more rapidly than the growth of the largest Lyapunov exponent for $\tau \geq 2$ days in all the cases (a)∼(d).

Figure 6 shows the distribution of α ($\tau = 3$ days) on each asymptotic solution (attractor) projected onto the ψ_3^0 - ψ_5^0 plane in the 25-dimensional phase space. Red dots indicate a relatively large α while blue ones small α. In the case of (a), the homoclinic-like trajectory is clearly seen; it recurrently approaches the S6(US) denoted by the symbol • and departs from it in the direction denoted by an arrow. The Lorenz index α increases gradually while the trajectory passes near the US. Similar distributions of α on each attractor are observed for larger ρ, (b)∼(d), although the homoclinic-like orbit becomes obscure as ρ increases. Gradual increase of α near M4 (MIN) denoted by the symbol • is still observed, because the trajectory goes counterclockwise on this plane.

To see the relation between α and the MP(S6 or M4) more clearly, in Fig. 7 we show the relation between $\alpha(\tau = 3$ days) and the distance of the initial states $\boldsymbol{x}(t_0)$ from the MP for 10 periods during which the trajectory approaches the MP most closely in the 9950-day period. The relation in the case of (a) is very similar for the 10 periods; α gradually increases while the trajectory approaches the US and departs from it. The nearest distance becomes large as ρ increases. However, there still remains the tendency that α gradually increases during the QS state. This tendency reminds us of the

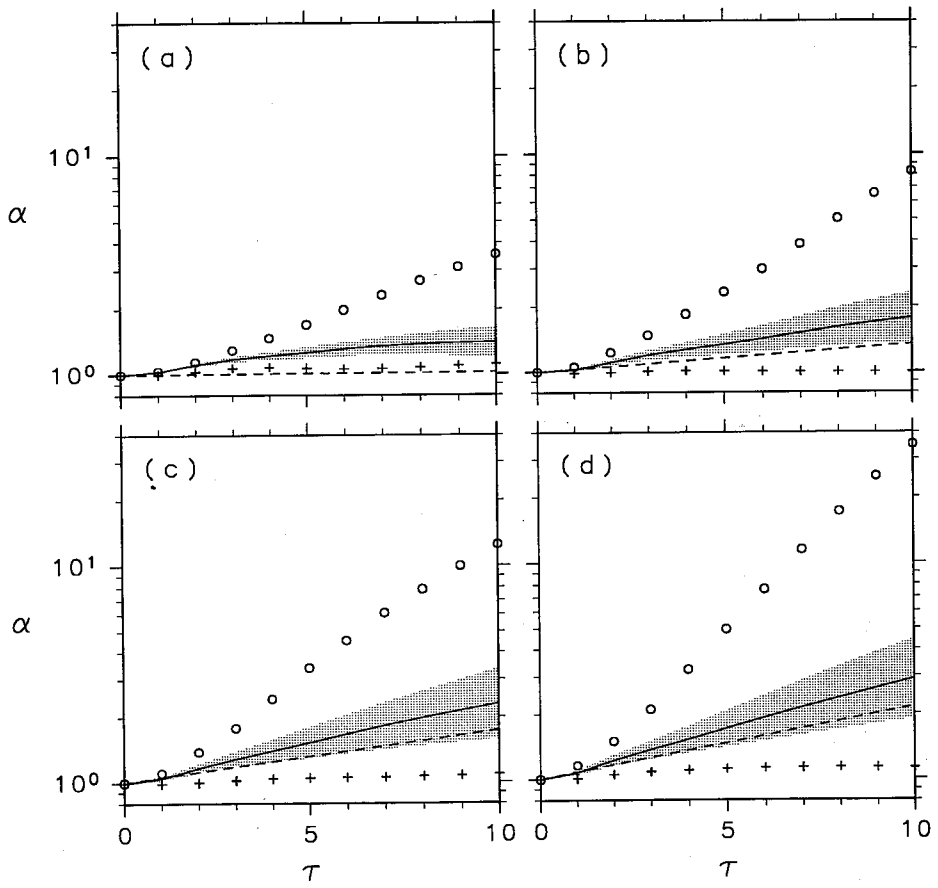

Fig. 5. Statistics of time-variations of the Lorenz index α along the solution of 9960-day period. The abscissa denotes the time interval τ. The geometric mean is indicated by a solid line. The shaded area is the range of [mean]$\pm$1$\times$[standard deviation]. Symbols $\circ$ and $+$ show the maximum and the minimum, respectively. The error growth with the largest Lyapunov exponent is also shown by a broken line. (a)$\sim$(d) are the same as those indicated in Fig. 3.

relation between α and QS states in one-dimensional systems.

In accordance with the theory developed in Section 2.4, α may vary in more than one manner around the MP depending on each trajectory as shown in Fig. 1, because the chaotic solutions for $\rho > 0.190$ satisfy $\|\boldsymbol{f}_{\rm MP}\| \ll \|{\rm J}_{\rm MP}(\boldsymbol{x} - \boldsymbol{x}_{\rm MP})\|$ during the QS states. However, Fig. 7 shows only one relation between α and MP.

In order to examine details of the relation between α and QS states obtained in the LG model, an additional experiment is done for the case of $\rho = 0.250$. Randomly 1000 initial points are chosen around the MP(M4) with a small distance of 6×10^{-3} and integrated numerically forward and backward for 50 days. Each trajectory satisfies the inequality $\|\boldsymbol{f}_{\rm MP}\| \ll \|{\rm J}_{\rm MP}(\boldsymbol{x} - \boldsymbol{x}_{\rm MP})\|$ during the QS states. All the four relations between α and the QS state as shown in Fig. 1 are obtained in the 1000 samples of the random trajectories around M4. However, the four relations are not observed with an equal probability. An ensemble average of the time-variation of the distance from the MP is shown by a broken line in Fig. 8a with a shaded area for [average]$\pm$1$\times$[standard deviation], and that of α in Fig. 8b. On average, α has a minimum when the trajectory is close to the MP around $t = 0$.

To compare this tendency of randomly chosen trajectories near the M4 with that of the trajectories on the chaotic attractor, 1000 samples of the trajectories close to the M4 are obtained by much longer time-integrations of 10^6 days. The time-variations of the distance from the M4 and α are shown by thick solid lines in Fig. 8 with a shaded area for one standard deviation. The distance of the trajectories on the attractor is statistically much smaller than that for the random case for $t < 0$ when it approaches the MP. In other words, the trajectory obtained in chaotic solutions approaches the M4 more slowly and the QS state persists for much longer time than that estimated from the random trajectories around the MP. The trajectory for the random case seems to be absorbed into the attractor along the forward time-integrations and, on the contrary, to be re-

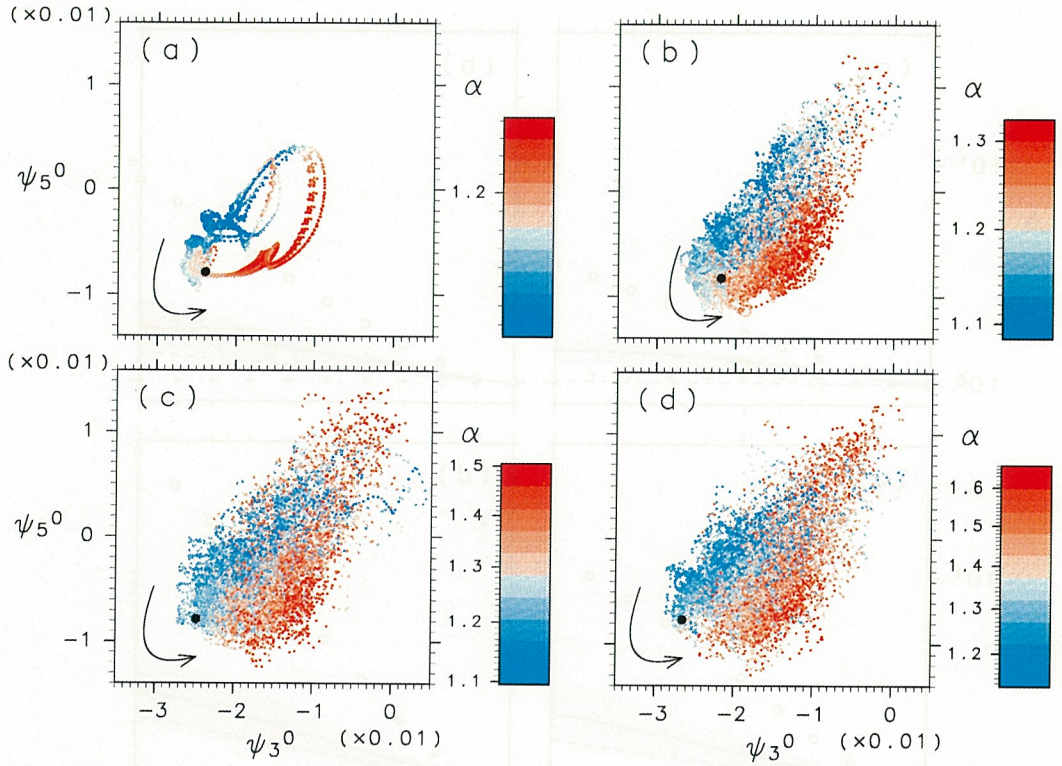

Fig. 6. Distribution of the Lorenz index α on the asymptotic solutions. The solutions are projected onto the ψ_3^0 - ψ_5^0 plane in 25-dimensional phase space. The symbol • denotes the MP; (a)S6, (b)∼(d)M4. Color bars are for the Lorenz index of $\tau = 3$ days. Arrows show the direction of the trajectory. (a)∼(d) are the same as those indicated in Fig. 3.

pelled from it along the backward time-integrations. The Lorenz index α observed in chaotic solutions is also statistically much smaller than that for the random trajectories for $t < 0$; α has a tendency to increase monotonically during the QS states in chaotic solutions. Because the trajectory of the chaotic solution is restricted on the attractor whose dimension is smaller than that of phase space, the direction in which the chaotic solution approaches the MP and departs from it is limited, unlike the case of random trajectories. As a result, there exists significant difference statistically between the two cases.

4. Concluding remarks

Relation between the Lorenz index α and MPs is investigated with simple non-linear systems. In one-dimensional systems there is a unique relation that α increases monotonically during a QS state, when the trajectory approaches a MIN and departs from it. However, in multi-dimensional systems there is no such unique relation between α and MPs. An example of non-linear two-dimensional system is given to show four different relations. During a QS state related to US as shown in Fig. 1, α increases monotonically, decreases monotonically, has a maximum, or has a minimum, depending on the trajectory. Similarly, during QS states related to MIN, on the assumption that the trajectory exists close enough to the MIN, α shows one of the four relations depending on the property of each MIN.

In the LG model with 25 variables only the same relation as one-dimensional systems is observed during the QS states related to MPs in the chaotic solutions for $\rho > 0.190$ (Fig. 7). A unique relation between α and the MP can be understood by the following reasoning. Since the distribution of the initial states chosen along the chaotic solution is restricted on the attractor in phase space unlike random distributions, the approach and departure of the solution is almost limited to one direction for each MP. Therefore, one of four types of behavior 1∼4 in Fig. 1, which were treated equally in Section 2.3, will be selected for each MP.

The relation indicated by Mukougawa *et al.* (1991) that the Lorenz index increases during the QS state, which is defined on the Poincaré section, in the Lorenz system with three variables is also understood in the same way. In this case, the operation of the Poincaré mapping makes a two-dimensional discrete dynamical system from the three-dimensional continuous dynamical system. The investigation of the local structure around the MIN, which is defined with the Poincaré map, will show that the Lorenz index α may vary in more than one manner during

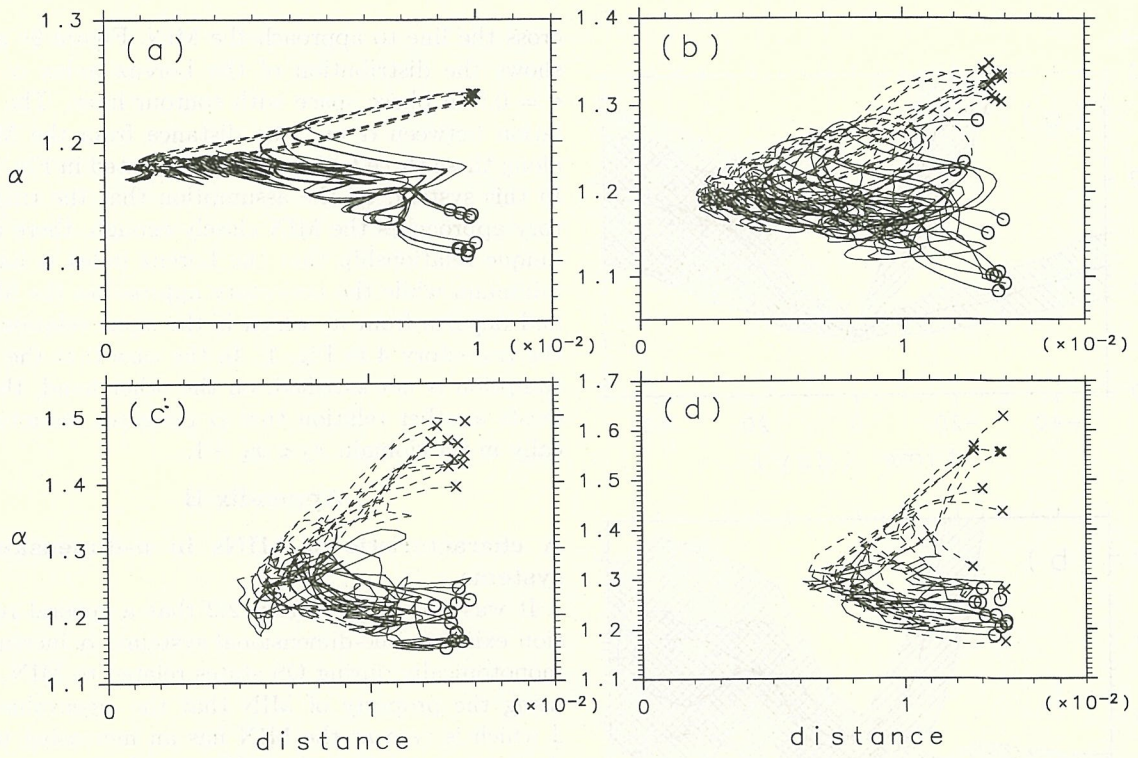

Fig. 7. Relation between the Lorenz index $\alpha(\tau = 3$ days) and the distance from the MP; (a) S6, (b)~(d) M4. For each solution of the 9950-day period, 10 periods are chosen during which the trajectory approaches the MP most closely; the approaching trajectories is indicated by solid lines and the departing trajectories by broken lines. Similar to those in Fig. 1b, symbols ○ and × show initial and last point of each period, respectively. (a)~(d) are the same as those indicated in Fig. 3.

the QS state. However, the same relation as one-dimensional systems is observed for the trajectory on the attractor.

Another relation between the Lorenz index α and MP(US) can be found in the Lorenz (1963) system. Mukougawa *et al.* (1991) also calculated α on the attractor of the Lorenz system. Their result (see their Fig. 7) shows that the closer to the US $(0,0,0)^{\mathsf{T}}$ the initial state $\boldsymbol{x}(t_0)$ is, the larger the value of α becomes. Therefore, there is the same relation as the behavior denoted by 2 in Fig. 1 that the Lorenz index α has a maximum when the trajectory is closest to the US.

Therefore, it seems reasonable to conclude that the relation obtained in the chaotic solutions of the LG model is coincident with the relation in one-dimensional systems by chance, just one of four possibilities. However, on the other hand, it is possible to assume that this relation is one of the necessary conditions of the recurrent QS states because it is difficult for the trajectory to approach the MP frequently under the condition of large α. Why this particular relation is selected in the chaotic solutions of the LG model is an unsettled question. Introduction of new dynamical concept and further study are necessary to answer the question.

Acknowledgment

We thank Dr. K. Ishioka for his FORTRAN code on the interaction coefficient method to compute the Jacobian terms. We also thank Professor H. Mukougawa and an anonymous reviewer for helpful suggestions and comments. The computations were done on the KDK system at Radio Atmospheric Science Center, Kyoto University. GFD-DENNOU Library was used for drawing the figures.

Appendix A

Local structure around MIN

We consider the local structure around MIN using the following two-dimensional system:

$$\begin{pmatrix}\dot{x}_1\\ \dot{x}_2\end{pmatrix} = \begin{pmatrix}1\\0\end{pmatrix} + \begin{pmatrix}0 & 0\\ 1 & -1\end{pmatrix}\begin{pmatrix}x_1\\ x_2\end{pmatrix} + \begin{pmatrix}\frac{1}{10}x_2^2\\ 0\end{pmatrix}, \quad \text{(A1)}$$

which has a MIN at the origin; $\boldsymbol{x}_{\mathrm{MP}} = (0,0)^{\mathsf{T}}$. The right-hand side of this equation consists of three terms: a constant term, a linear term and a quadratic term. The flow field of the constant term and the linear term in phase space are shown in Figs. 9a and 9b, respectively. The constant term allows the trajectory to approach the MIN along only one direction of $\boldsymbol{f}_{\mathrm{MP}}$, while the linear term allows

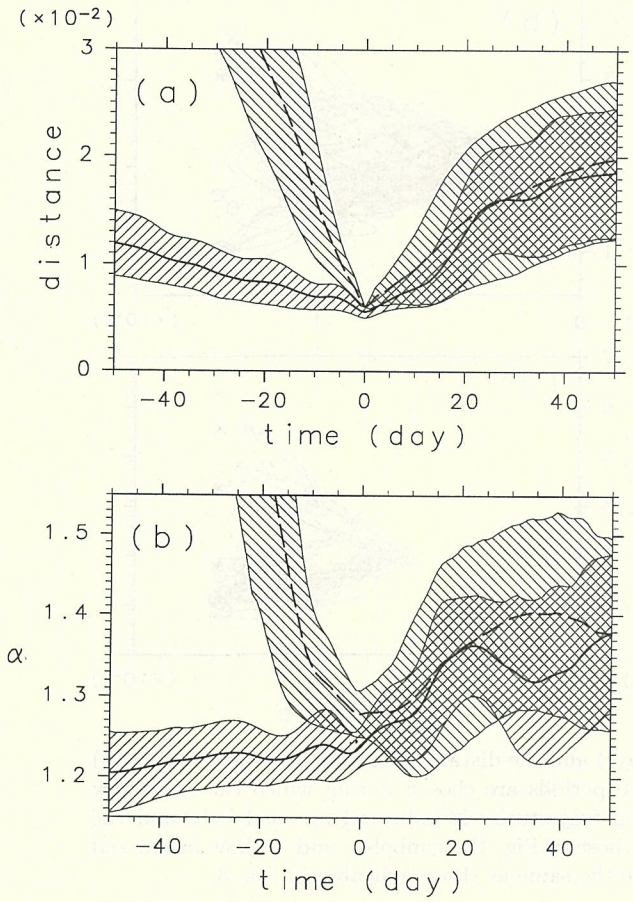

Fig. 8. Statistics of temporal variations of (a) the distance from the MP(M4) and (b) the Lorenz index $\alpha(\tau = 3$ days) for $\rho = 0.250$. Thick solid line is an ensemble average of 1000 samples of trajectories on the attractor, while broken line is that for random trajectories. Shaded area means [average]$\pm 1\times$[standard deviation].

two directions which are both parallel to the stable eigenvector, $(0,1)^{\mathsf{T}}$, of the coefficient matrix of the linear term J_{MP}. Therefore, in the case that the inequality $\|\boldsymbol{f}_{\mathrm{MP}}\| \ll \|\mathsf{J}_{\mathrm{MP}}\boldsymbol{x}\|$ is satisfied for any time, the trajectory can approach the MIN along either of the two directions given by the linear term. On the other hand, in the case that the inequality $\|\boldsymbol{f}_{\mathrm{MP}}\| \gg \|\mathsf{J}_{\mathrm{MP}}\boldsymbol{x}\|$ is satisfied for some time period, the direction of approach is fixed in one direction given by the constant term.

Figure 9c shows the total flow field of Eq. (A1) and three trajectories which approach the MIN closely enough to satisfy the inequality $\|\boldsymbol{f}_{\mathrm{MP}}\| \gg \|\mathsf{J}_{\mathrm{MP}}\boldsymbol{x}\|$. All the initial points exist in the same quadrant and the trajectories approach the MIN along the fixed direction. Indeed, when the quadratic term can be neglected, trajectories whose initial point is in the domain under a straight line $x_2 = x_1 - 1$ can not cross the line to approach the MIN. Figure 9c also shows the distribution of the Lorenz index α for $\tau = 0.5$ in phase space with contour lines. The relation between α and the distance from the MIN along these three trajectories is indicated in Fig. 9d. In this system, on the assumption that the trajectory approaches the MIN closely enough, there is a unique relationship that the Lorenz index α has a minimum while the trajectory approaches the MIN and departs from it, which is the same relation as the trajectory 4 in Fig. 1. In the case that the assumption is not satisfied, on the other hand, there exists another relation that α increases monotonically in the domain $x_2 < x_1 - 1$.

Appendix B

A characteristic of MINs in n-dimensional systems

It was shown in Section 2.2 that a general relation exists in one-dimensional systems: α increases monotonically during QS states related to MIN, by using the property of MIN that the eigenvalue of J which is zero at the MIN has an increasing tendency along the trajectory. Here we shall present an equation which gives the time tendency of a specific eigenvalue of J at a MIN in general n-dimensional systems. The eigenvalue takes a value of zero at the MIN.

In the n-dimensional dynamical system governed by Eq. (1), MIN is defined as a point which satisfies the following three conditions(Mukougawa, 1988): (i) $F \equiv \|\boldsymbol{f}\|^2 \neq 0$, (ii) $\nabla F = 2\mathsf{J}^{\mathsf{T}}\boldsymbol{f} = \mathbf{o}$, (iii) the Hessian matrix H of $F(H_{ij} = \partial^2 F/\partial x_i \partial x_j)$ is positive definite. The conditions (i) and (ii) show that the matrix $\mathsf{J}_{\mathrm{M}}^{\mathsf{T}}$ has a zero-eigenvalue and the corresponding eigenvector $\boldsymbol{f}_{\mathrm{M}}$, where subscript $_{\mathrm{M}}$ indicates the value at the MIN.

We consider the variation of one eigenvalue λ of the matrix J^{T}, which is zero at MIN, along the trajectory of the solution passing through the MIN. Let $\boldsymbol{v}$ be the eigenvector corresponding to λ such that $\boldsymbol{v}_{\mathrm{M}} = \boldsymbol{f}_{\mathrm{M}}$, the equation of the relation between λ and $\boldsymbol{v}$ is $\mathsf{J}^{\mathsf{T}}\boldsymbol{v} = \lambda\boldsymbol{v}$. By differentiating this equation with respect to time t and considering the state at $t = t_{\mathrm{M}}$, at which $\boldsymbol{x} = \boldsymbol{x}_{\mathrm{M}}$, $\lambda = 0$ and $\boldsymbol{v} = \boldsymbol{f}_{\mathrm{M}}$, we obtain

$$\left.\frac{d\mathsf{J}^{\mathsf{T}}}{dt}\right|_{t=t_{\mathrm{M}}} \boldsymbol{f}_{\mathrm{M}} + \mathsf{J}_{\mathrm{M}}^{\mathsf{T}} \left.\frac{d\boldsymbol{v}}{dt}\right|_{t=t_{\mathrm{M}}} = \left.\frac{d\lambda}{dt}\right|_{t=t_{\mathrm{M}}} \boldsymbol{f}_{\mathrm{M}}. \quad \text{(B1)}$$

By the way, the following relation exists:

$$\frac{d\mathsf{J}^{\mathsf{T}}}{dt}\boldsymbol{f} = \frac{1}{2}\mathsf{H}\boldsymbol{f} - \mathsf{J}^{\mathsf{T}}\mathsf{J}\boldsymbol{f}. \quad \text{(B2)}$$

Equation (B2) is confirmed by considering the component of the matrices as follows:

$$(\mathsf{H})_{ij} = \sum_{k=1}^{n} \frac{\partial^2 f_k^2}{\partial x_i \partial x_j} = 2\sum_{k=1}^{n}\left(\frac{\partial f_k}{\partial x_i}\frac{\partial f_k}{\partial x_j} + f_k \frac{\partial^2 f_k}{\partial x_i \partial x_j}\right)$$

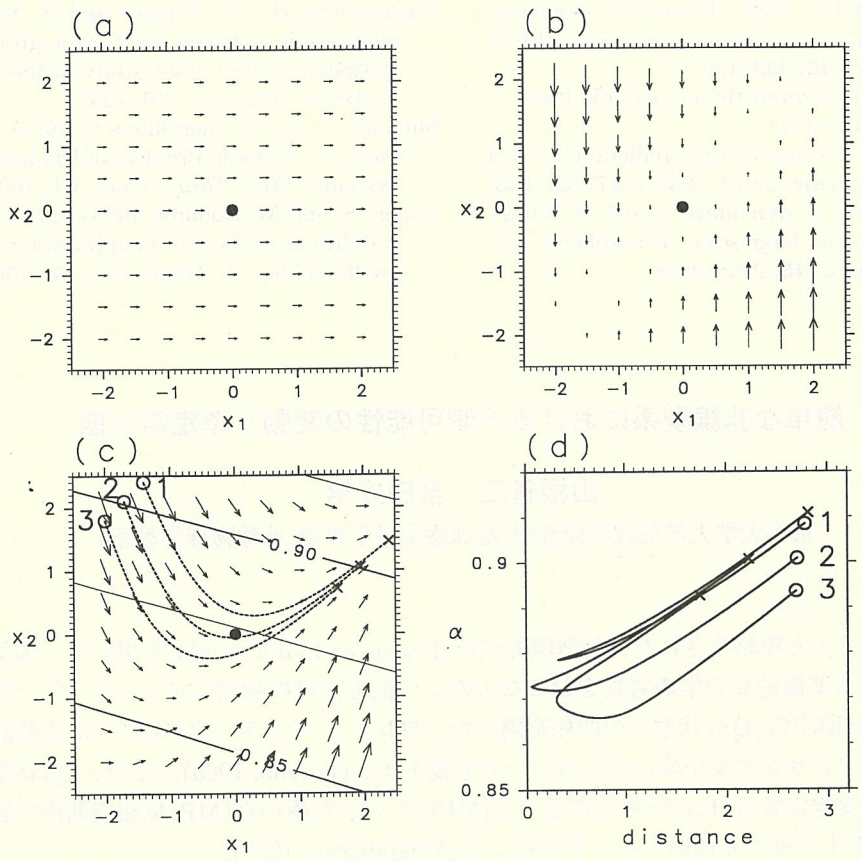

Fig. 9. (a) Flow field of the constant term of Eq. (A1). The MIN $(0,0)^{\mathsf{T}}$ is denoted by •. (b) The same as (a) but the linear term. (c) Distribution of the Lorenz index α for $\tau = 0.5$. Arrows show the total flow field of Eq. (A1). Three trajectories $x(t)$ are drawn with broken lines from initial points denoted by ○ to final points at $t = 3.5$ denoted by ×. (d) Relation between the Lorenz index $\alpha(\tau = 0.5)$ and the distance of the solution from the MIN. Numbers and markers are the same as those indicated in (c).

$$= 2(\mathsf{J}^{\mathsf{T}}\mathsf{J})_{ij} + 2\sum_{k=1}^{n} f_k \frac{\partial^2 f_k}{\partial x_i \partial x_j},$$

and

$$\left(\frac{d\mathsf{J}^{\mathsf{T}}}{dt}\right)_{ij} = \frac{d}{dt}\frac{\partial f_j}{\partial x_i} = \sum_{k=1}^{n} \frac{dx_k}{dt}\frac{\partial}{\partial x_k}\frac{\partial f_j}{\partial x_i}$$
$$= \sum_{k=1}^{n} f_k \frac{\partial^2 f_j}{\partial x_k \partial x_i}.$$

Substituting Eq. (B2) into Eq. (B1) yields

$$\frac{1}{2}\mathsf{H}_{\mathrm{M}}\boldsymbol{f}_{\mathrm{M}} - \mathsf{J}_{\mathrm{M}}^{\mathsf{T}}\mathsf{J}_{\mathrm{M}}\boldsymbol{f}_{\mathrm{M}} + \mathsf{J}_{\mathrm{M}}^{\mathsf{T}}\left.\frac{d\boldsymbol{v}}{dt}\right|_{t=t_{\mathrm{M}}} = \left.\frac{d\lambda}{dt}\right|_{t=t_{\mathrm{M}}} \boldsymbol{f}_{\mathrm{M}}. \tag{B3}$$

In one-dimensional systems Eq. (B3) is reduced to $\frac{1}{2}\mathsf{H}_{\mathrm{M}} = \left.\frac{d}{dt}\frac{df}{dx}\right|_{t=t_{\mathrm{M}}}$ because $\lambda = \mathsf{J} = df/dx$ and $\mathsf{J}_{\mathrm{M}} = 0$; this equation is the same as was obtained in Section 2.2. Let $\boldsymbol{u}$ be the eigenvector of J corresponding to the eigenvalue λ, and let $\boldsymbol{u}_{\mathrm{M}}^{\mathsf{T}}$ operate on Eq. (B3) to the left, then the following equation is obtained:

$$\left.\frac{d\lambda}{dt}\right|_{t=t_{\mathrm{M}}} = \frac{\boldsymbol{u}_{\mathrm{M}}^{\mathsf{T}}\mathsf{H}_{\mathrm{M}}\boldsymbol{f}_{\mathrm{M}}}{2\boldsymbol{u}_{\mathrm{M}}^{\mathsf{T}}\boldsymbol{f}_{\mathrm{M}}}. \tag{B4}$$

Equation (B4) shows that in one-dimensional systems $\left.\frac{d\lambda}{dt}\right|_{t=t_{\mathrm{M}}} = \frac{1}{2}\mathsf{H}_{\mathrm{M}} > 0$ because H_{M} is positive definite. In multi-dimensional systems, however, the sign of $\left.\frac{d\lambda}{dt}\right|_{t=t_{\mathrm{M}}}$ is generally indeterminate except for a case that J is symmetric matrix, in which $\left.\frac{d\lambda}{dt}\right|_{t=t_{\mathrm{M}}} > 0$ because $\boldsymbol{u}$ is parallel to $\boldsymbol{v}$. Thus, the unique relation $\left.\frac{d\lambda}{dt}\right|_{t=t_{\mathrm{M}}} > 0$ in one-dimensional systems does not hold generally in multi-dimensional systems.

References

Kimoto, M., H. Mukougawa and S. Yoden, 1992: Medium-range forecast skill variation and blocking transition: A case study. *Mon. Wea. Rev.*, **120**, 1616–1627.

Legras, B. and M. Ghil, 1985: Persistent anomalies, blocking and variations in atmospheric predictability. *J. Atmos. Sci.*, **42**, 433–471.
Lorenz, E.N., 1963: Deterministic nonperiodic flow. *J. Atmos. Sci.*, **20**, 130–141.
Lorenz, E.N., 1965: A study of the predictability of a 28-variable atmospheric model. *Tellus*, **17**, 321–333.
Mukougawa, H., 1988: A dynamical model of "quasi-stationary" states in large-scale atmospheric motions. *J. Atmos. Sci.*, **45**, 2868–2888.
Mukougawa, H., M. Kimoto and S. Yoden, 1991: A relationship between local error growth and quasi-stationary states: Case study in the Lorenz system. *J. Atmos. Sci.*, **48**, 1231–1237.
Shimada, I. and T. Nagashima, 1979: A Numerical Approach to Ergodic Problem of Dissipative Dynamical Systems. *Prog. Theor. Phys.*, **61**, 1605–1616.
Yoden, S. and M. Nomura, 1993: Finite-time Lyapunov stability analysis and its application to atmospheric predictability. *J. Atmos. Sci.*, **50**, 1531–1543.

簡単な非線型系における予測可能性の変動と準定常状態

山根省三・余田成男
（京都大学大学院理学研究科 地球惑星科学専攻 地球物理学教室）

低次元の概念モデルと簡略化された大気循環モデル (Legras and Ghil, 1985) を用いて、大気予測可能性の時間変動に関する基礎的な力学の考察をおこなった。予測可能性の指標にロレンツ インデックス α を用いて、αの変動と準定常 (QS) 状態との関係を調べた。ロレンツ インデックスαは、ある期間における微小擾乱の成長率をアンサンブル平均したものとして定義される (Lorenz, 1965)。また、QS状態は、解軌道が位相空間内で不安定定常解 (US) や非定常極小点 (MIN) といった極小点（MP; 位相空間内で解軌道の速さが極小となる点）のすぐ近くを通過するときに起こる (Mukougawa, 1988)。

一次元力学系では、MINに関連するQS状態の期間中αが単調に増加するという決まった関係が存在する。しかし、多次元力学系では、αとQS状態との間にはそのような関係は存在しない。USに関連するQS状態の期間中、αは個々の軌道に依存して、単調に増加、または減少、あるいは極大、または極小を持つ。更に、軌道がMINに十分近づくという仮定のもとでは、MINに関連するQS状態の期間中、αは上で述べた4つの関係のうちの1つをそのMIN固有の関係として示す。

アトラクター上の軌道を考えれば、MPに関連したいずれのQS状態も、4つの関係のうちの1つをそのMP固有の関係として持つ。Legras and Ghilモデルのカオス解では、一次元力学系と同じようにQS状態の期間中にαが単調に増加する関係が見られた。ただし、両者の一致は4つの可能性の1つに過ぎないと考えられる。